

Selective methoxylation of α -pinene to α -terpinyl methyl ether over Al^{3+} ion-exchanged clays

CATRINESCU, C., FERNANDES, C., CASTILHO, P. and BREEN, C.

Available from Sheffield Hallam University Research Archive (SHURA) at:

<http://shura.shu.ac.uk/13336/>

This document is the author deposited version. You are advised to consult the publisher's version if you wish to cite from it.

Published version

CATRINESCU, C., FERNANDES, C., CASTILHO, P. and BREEN, C. (2015). Selective methoxylation of α -pinene to α -terpinyl methyl ether over Al^{3+} ion-exchanged clays. *Applied Catalysis A: General*, 489, 171-179.

Repository use policy

Copyright © and Moral Rights for the papers on this site are retained by the individual authors and/or other copyright owners. Users may download and/or print one copy of any article(s) in SHURA to facilitate their private study or for non-commercial research. You may not engage in further distribution of the material or use it for any profit-making activities or any commercial gain.

1 **Selective methoxylation of α -pinene to α -terpinyl methyl ether over Al^{3+} ion-**
2 **exchanged clays**

3 C. Catrinescu^{a,b,*}, C. Fernandes^{a,c}, P. Castilho^a, C. Breen^d

4 ^aCentro de Química da Madeira(CQM), Centro de Ciências Exactas e da Engenharia
5 da Universidade da Madeira, Campus Universitário da Penteada, 9000-390 Funchal,
6 Portugal

7 ^b“Gheorghe Asachi” Technical University of Iasi, Faculty of Chemical Engineering
8 and Environmental Protection, Department of Environmental Engineering and
9 Management, 73 D. Mangeron Blvd, 700050 Iasi, Romania

10 ^cLaboratório Regional de Engenharia Civil, Rua Agostinho Pereira de Oliveira, 9000-
11 264 Funchal

12 ^dMaterials and Engineering Research Institute, Sheffield Hallam University, Howard
13 Street, Sheffield, S1 1WB, UK

14

15 **Abstract**

16 In this study, we report the use of clay-based catalysts in the methoxylation of α -
17 pinene, for the selective synthesis of α -terpinyl methyl ether, TME. The main reaction
18 products and intermediates were identified by GC-MS. The reaction conditions
19 (stirring rate and catalyst load) that afford a kinetic regime were established. SAz-1
20 (Cheto, Arizona, USA) source clay and a montmorillonite (SD) from Porto Santo,
21 Madeira Archipelago, Portugal, were modified by ion-exchange with Al^{3+} to produce
22 catalysts with markedly different acidities and textural properties. The catalysts based
23 on the high layer-charge SAz-1 montmorillonite proved to be the most active. Ion-
24 exchange with Al^{3+} , followed by thermal activation at 150 °C, afforded the highest
25 number of Brønsted acid sites - a significant proportion of which were located in the
26 clay gallery - and this coincided with the maximum catalytic activity. The influence of
27 various reaction conditions, to maximize α -pinene conversion and selectivity, was
28 studied over AISAz-1. When the reaction was performed for 1h at 60 °C, the
29 conversion reached 65% with 65 % selectivity towards the mono-ether, TME. Similar
30 conversions and selectivities required up to 50 hours over zeolites and other solid acid
31 catalysts. The kinetic dependencies of this reaction on temperature and reagent
32 concentration, over the selected clays were also investigated. It was established that,
33 in the temperature and reagent concentration regime studied, the reaction was first
34 order with respect to α -pinene. The apparent activation energies over the two
35 catalysts, calculated from Arrhenius plots, were almost identical at 72 kJ mol⁻¹.

36

37 Keywords: Ion-exchanged clays, clay acidity, catalysis, pinene, methoxylation,

38 terpinyl methyl ether

39 **1. Introduction**

* Corresponding author. Tel.: +40 232 237594; Fax: +40 232 237594.

E-mail address: ccatrine@ch.tuiasi.ro (C. Catrinescu)

1 The use of renewable feedstocks, such as monoterpenoids, to produce fine chemicals
2 *via* heterogeneous catalytic processes is considered a sustainable approach which
3 conforms with the principles of green chemistry [1]. Terpenes, such as limonene and
4 pinene, are an abundant renewable feedstock, used as starting materials for the
5 synthesis of fine chemicals, in food, cosmetic and pharmaceutical industries. Terpenes
6 are found not only in several essential oils but also as the major constituents of pine
7 resins and of some byproducts of the pulp, paper and food (citrus) industries [2,3].
8 Pinene is a natural bicyclic monoterpene that can be separated, by steam distillation,
9 from gum and sulphate turpentine which presents two structural isomers (α - and β -).
10 α -pinene is the most widely encountered terpenoid in nature [2] and finds numerous
11 uses in the food, fragrance and pharmaceutical sectors as well as in the synthesis of
12 chemical intermediates. Thus, α -pinene is considered a versatile building block for
13 the synthesis of high-value added chemicals, mainly through catalytic processes, such
14 as isomerization, epoxidation and pinene oxide isomerization, hydration and
15 dehydroisomerization, esterification, etherification [2-4] and also in a four-step
16 synthesis of linalool from α -pinene [6, 10]. The alkoxylation of pinene is a less
17 explored route to produce *1-methyl-4-(α -alkoxyisopropyl)-1-cyclohexenes*. These
18 compounds are used as flavours and fragrances for perfume and cosmetic products, as
19 additives for pharmaceuticals and agricultural chemicals, and also in the food
20 industry. Among these functionalized monoterpenes, the α -terpinyl methyl ether is of
21 commercial interest due to its pleasant grapefruit-like aroma. This compound is
22 conventionally produced via the alkoxylation of pinene or limonene using mineral
23 acids. The use of strong homogeneous liquid acids is not recommended for industrial
24 applications due to the associated corrosion and environmental challenges. Previous
25 studies on α -pinene and limonene methoxylation have been principally performed

1 using zeolites [7] although clay- based catalysts can also be used [8]. The alkoxylation
2 of limonene over β zeolite and ion-exchanged clays afforded good yields (around
3 85%) whereas the methoxylation of pinene, over the same β zeolite, gave lower yields
4 (50 %) of the same product. The methoxylation of pinene has been also studied over
5 acidic cation exchange resins [9] and sulfonic acid-modified mesoporous silica [10].
6 However, more recent studies over poly(vinyl alcohol) containing sulfonic acid
7 groups [11], heteropolyacids immobilized on silica [12] and microporous and
8 mesoporous carbons [13] reported good selectivities, of ca. 60%, at almost complete
9 conversion.

10 Clay minerals, which are natural materials that cost significantly less than the
11 catalysts listed above, are versatile and environmentally friendly catalysts that can be
12 modified with relative ease to promote a wide variety of organic reactions [14].

13 Beside the type of clay, the nature, the locality and the extent of the isomorphous
14 substitution strongly influences the layer charge of the clay and exerts a major
15 influence on the acidity and accessibility of the active sites. These intrinsic
16 characteristics of the clays, responsible for their catalytic activity, can be readily
17 improved using different methods such as *ion-exchange*, *acid treatment* and *pillaring*
18 [15]. Thus, Ni^{2+} - and Al^{3+} -exchanged montmorillonites, following appropriate thermal
19 activation procedures, are considered model Lewis and Brønsted acids, respectively.

20 The nature of the active sites has been unequivocally determined using FT-IR spectra
21 of adsorbed pyridine [16] and verified by catalytic data.

22 In this work we report the synthesis of α -terpinyl methyl ether via the methoxylation
23 of α -pinene over clay catalysts. Based on our recent results detailing the
24 methoxylation of limonene [8], two starting clays, with different compositions and
25 properties, were selected and these were activated by ion-exchange with Al^{3+} and then

1 thermally activated at 150 °C. This approach is known to afford the maximum
2 catalytic activity in Brønsted acid catalyzed organic reactions involving polar
3 reagents.

4

5 **2. Experimental**

6

7 *2.1 Catalyst preparation*

8

9 SAz-1 (Cheto, Arizona, USA), received from The Clay Mineral Society Source Clay
10 repository (Purdue University), was suspended in deionized water and the < 2 μm size
11 fraction was collected by centrifugation. The raw bentonite (SD) was collected from
12 the Serra de Dentro deposit (Porto Santo - Madeira Archipelago, Portugal) and
13 purified [18] to give the Na-exchanged form (NaSD). The major impurities were
14 removed by low speed centrifugation (6 min. At 600 rpm), to obtain the < 2 μm size
15 fraction, followed by the removal of inorganic carbonates by incremental addition of a
16 0.5 M sodium acetate buffer until the clay suspension reached pH 6.8. Then, the
17 product was converted into the Na-exchanged form using 1M aqueous sodium
18 chloride solution. Excess Cl⁻ was removed by dialysis and the solid clay was obtained
19 after drying the gel collected following centrifugation at 4500 rpm for 30 min. The
20 chemical composition for SAz-1 and NaSD is reported in Table 1.

21

22 Table 1. Elemental composition for the purified host clays and for the Al³⁺ ion-
23 exchanged forms.

24

25 SAz-1 and NaSD were treated three times with 0.3 M Al(NO₃)₃, washed, dried and

1 ground to give the AlSAz-1 and AlSD catalysts. These samples were stored in a
2 desiccator over saturated aqueous $\text{Ca}(\text{NO}_3)_2$.

3

4 *2.2 Characterization*

5

6 The XRD patterns were recorded using a Shimadzu LabX XRD-6000 diffractometer
7 with $\text{Cu K}\alpha$ radiation ($\lambda = 1.54184 \text{ \AA}$). The nitrogen adsorption-desorption isotherms at
8 $-196 \text{ }^\circ\text{C}$ were determined on an Autosorb iQ from Quantachrome Instruments,
9 equipped with turbomolecular pumps for high vacuum attainment, using helium (for
10 dead space calibration) and nitrogen of 99.999% purity. Prior to the adsorption
11 measurements, all the samples were outgassed for 5h at $200 \text{ }^\circ\text{C}$, achieved using a
12 heating rate of $1 \text{ }^\circ\text{C min}^{-1}$.

13 TG data were recorded on a Mettler TG50 thermobalance equipped with a TC10A
14 processor. Samples ($\sim 10\text{mg}$) were transferred directly out of cyclohexylamine (CHA)
15 vapour into the thermobalance and the desorption traces were recorded at a heating
16 rate of 20°C under a nitrogen flow of $25 \text{ cm}^3/\text{min}$. Samples were conditioned for 15
17 min under flowing nitrogen to reduce the amount of physisorbed CHA. Variable
18 temperature diffuse reflectance infrared Fourier transform spectra (VT-DRIFTS),
19 were recorded at room temperature, then at $25 \text{ }^\circ\text{C}$ increments until 250°C . Samples
20 were held at a specific temperature for 15 min in a flow of dry nitrogen in a variable-
21 temperature cell (Graseby-Specac; maximum operating temperature 500°C). The
22 spectrometer used was a Mattson Polaris operating at 4 cm^{-1} resolution and 256 scans.

23

24 *2.3 Catalytic tests*

25 α -pinene and n-decane (internal standard) received from Sigma Aldrich were dried

1 over anhydrous magnesium sulphate prior to use. Anhydrous methanol was used as
2 received from Sigma Aldrich. The reactions were performed in a stirred 25 ml batch
3 reactor, equipped with a reflux condenser, under drying tube (CaCl_2) protection.
4 Before the reaction, a known amount of catalyst was thermally activated at $150\text{ }^\circ\text{C}$, in
5 air, for 2 h in a vial. Before being removed from the oven, the vials were stoppered
6 and then placed in a desiccator to cool and prevent rehydration. After being cooled at
7 room temperature (15 min) the catalyst powder was quickly transferred into the
8 reaction vessel containing dry methanol, preheated at the reaction temperature. The
9 injection of pinene and n-decane (internal standard) marked the start of the reaction.
10 Samples were taken periodically and the catalyst was removed by syringe filtration.
11 The filter had no influence on the reaction products and no further reaction took place
12 during storage. The reaction products were identified by GC-MS (Agilent
13 6890N/MSD GC-MS system) and quantified by GC with FID, using a J&W
14 Carbowax 20M column and n-decane as an internal standard.
15 In a separate test the effect of the larger amounts of water available in non-thermally
16 activated clays was evaluated. These high water content samples were stored in a
17 desiccator over saturated aqueous $\text{Ca}(\text{NO}_3)_2$ prior to their use as a catalyst.
18 Initial reaction rates were calculated utilizing the concentration versus time data
19 collected during the first few minutes of the reaction. During this initial time period,
20 the concentration of the reactants decreased almost linearly with time, and hence the
21 reaction rate i.e., the differential of the reactant concentration with respect to time,
22 was calculated from the slope of a linear fit to these initial data.

23

24 **3. Results and discussion**

25 *3.1 Characterization*

1 The chemical analysis of the original and ion-exchanged clays (Table 1) confirmed
2 that SAz-1 contained a large amount of structural magnesium - located in the
3 octahedral sheet - and, in comparison to SD, exhibited a higher cation exchange
4 capacity (CEC) which reflected a higher layer charge. The purified SD sample is an
5 iron-rich clay that displayed a markedly higher specific surface area than SAz-1. The
6 most important results of the physical-chemical characterization are summarized in
7 Table 2.

8

9 Table 2. The main characteristics of the Al³⁺-exchanged clays

10

11 The XRD trace of the unpurified SD confirmed that the major components were
12 montmorillonite and magnesian calcite (C). Smaller amounts of anorthite (A),
13 feldspar (F) and quartz (Q) were present as impurities (Figure 1). However, most of
14 the impurities were removed during the purification step, as shown in the trace
15 obtained from NaSD. The powder XRD patterns of the Al³⁺-exchanged clays revealed
16 peaks corresponding to montmorillonites, with well defined d₀₀₁ reflections (5.96° 2θ,
17 14.8 Å), suggesting a well-ordered arrangement of the clay platelets, with two layers
18 of hydration water in the interlayer prior to activation at 150 °C.

19

20 Figure 1. The powder XRD patterns for raw, purified and Al³⁺-exchanged clays.
21 Impurities: magnesian calcite (C), anorthite (A), feldspar (F) and quartz (Q)

22

23 The textural properties of Al³⁺- exchanged clays were investigated using nitrogen
24 adsorption at -196 °C. The values of the specific surface areas, obtained by applying
25 the B.E.T. method [23] to the corresponding isotherms, are presented in Table 2.

1 These represent the accessible surface in the unswollen state of the clay and is
2 determined by the microporosity resulting from the quasi-crystalline overlap region
3 and from the accessible areas of the interlayer [8]. The total specific surface area
4 might also be affected, to a smaller extent, by the arrangement of the particles with
5 respect to each other (microstructure). Previous work revealed that the isotherms for
6 Al-SD and Al-SAZ-1 approached type IIb [8] and displayed hysteresis loops
7 associated with slit shaped pores between plate-shaped particles. The high surface
8 areas were attributed to the presence of narrow micropores [8].

9 The nature of the acid sites generated on the Al³⁺-exchanged clays were explored by
10 comparing the variable temperature diffuse reflectance infrared Fourier transform
11 spectra (VT-DRIFTS) of pyridine-treated samples and the number of sites were
12 estimated using thermal desorption (TG) of cyclohexylamine (CHA). In accordance
13 with our previous studies [8, 16, 20], Al³⁺-exchanged clays exhibited bands at 1635
14 and 1540 cm⁻¹ attributed to pyridinium ion, formed on Brønsted acid sites (BPYR),
15 and some minor bands at 1613 and 1450 cm⁻¹ that are diagnostic for pyridine co-
16 ordinally bound to Lewis acid sites (LPYR). The peaks at 1596 and 1440 cm⁻¹, in the
17 spectra recorded at lower temperatures, report the presence of H-bonded pyridine
18 (HPYR). All these species contribute to the intensity of the 1490 cm⁻¹ band although
19 the largest contribution at higher temperatures (> 120 °C) is from BPYR.

20

21 Figure 2 . VT-DRIFTS spectra of Al-SAZ-1 following exposure to pyridine vapour
22 and evacuation at (a) 50 °C, (b) 100 °C, (c) 150 °C, (d) 200 °C and (e) 250 °C.

23

24 The evolution of these diagnostic bands with temperature is presented in Figure 2.

25 The spectrum recorded at 50 °C for pyridine-treated Al³⁺-exchanged samples revealed

1 an already well-defined BPYR peak at 1539 cm^{-1} . This peak increased in intensity and
2 reached a maximum at $150\text{ }^{\circ}\text{C}$, then diminished progressively for activation at higher
3 temperatures. The continued presence of this band at $250\text{ }^{\circ}\text{C}$ highlighted the strength
4 of the Brønsted acid sites on Al^{3+} -exchanged clays. The spectrum of pyridine-treated
5 Al-SD at $150\text{ }^{\circ}\text{C}$ exhibited strong bands, diagnostic of pyridine bound to Brønsted
6 acid sites, at 1490 , 1540 and 1653 cm^{-1} [8, 16].

7 Thermal desorption of cyclohexylamine was used to quantify the number of the acid
8 sites on clay catalysts [16]. The technique determines the weight loss between 280
9 and $440\text{ }^{\circ}\text{C}$ and converts it to the number of mmol of CHA desorbed. The relative
10 ease of obtaining this quantity has popularised its use, even though the value obtained
11 does not readily distinguish between cyclohexylamine bound to Brønsted or Lewis
12 acid sites [20]. The quantity of CHA desorbed from Al-SD, in the appropriate
13 temperature interval (Table 2) was lower than that desorbed from Al-SAz-1, which
14 correlated well with the difference in CEC between SAz-1 ($120\text{ meq }100\text{ g}^{-1}$) and SD
15 ($81\text{ meq }100\text{ g}^{-1}$).

16 A significant difference between SAz-1 and SD is the extent of replacement of
17 aluminium by magnesium in the octahedral layer, resulting in different layer charges
18 which are identified by the different cation exchange capacities (CEC) and acidities,
19 as shown in the last two columns in Table 2. The location and the density of the layer
20 charge are the main characteristics that are expected to influence the catalytic activity,
21 provided that the interlayer space is accessible to the reagents.

22 **3.2 Catalytic tests**

23 *3.2.1 Potential mass transfer limitations*

24 A preliminary investigation was conducted to identify the experimental conditions
25 that ensure a true kinetic regime for the tests, i.e. the absence of external mass transfer

1 limitations. Initial rate measurements were carried out at different stirring rates,
2 catalyst loadings and temperatures. The extent of the external diffusion has been
3 verified by performing experiments at increasing stirring rates (100, 250, 500 and 750
4 and 1000 rpm at 60 °C). The reaction rate increased up to 500 rpm then approached
5 an asymptotic value beyond which the external mass transfer effects were negligible.

6

7 Figure 3. The influence of the catalyst load on the initial reaction rate over AlSAz-1
8 and AlSD. Inset: Early time behaviour. Reaction conditions: 10 ml methanol, 0.5 ml
9 pinene, 60 °C, 750 rpm

10

11 Having adopted a reaction temperature of 60 °C and a stirring rate of 750 rpm, the
12 kinetic regime was confirmed by performing experiments at increasing catalysts
13 loads. The absence of mass transfer limitations at this temperature also guaranteed
14 their absence at lower temperatures, where the reaction was slower. The experimental
15 results were plotted using $1/r = f(1/m)$ charts (Figure 3), where r is the reaction rate
16 and m is the mass of catalyst used [21, 22]. The plots were linear, for 0.50- 4.0 % w/v
17 range, and passed through the origin, confirming that the mass transfer resistance was
18 negligible in this range. The value of the reaction rate per unit catalyst mass (3×10^{-6}
19 $\text{mol s}^{-1} \text{g}^{-1}$) was constant over this interval and decreased to values below $2 \times 10^{-6} \text{ mol}$
20 s^{-1} at catalyst loadings in excess of 10 % w/v. Significantly lower reaction rates ($< 10^{-7}$
21 $\text{mol s}^{-1} \text{g}^{-1}$) were reported by Pito et al. [11,12] and Matos [13] in catalytic tests
22 performed over extended reaction time, of 30-60 hour.

23 3.2.2 Reaction products and intermediates

24 Scheme 1 illustrates the main reaction products and intermediates identified using
25 GC-MS (Supporting information). Pinene (1) reacted with methanol over the acid

1 sites available on the clay surface to form terpinyl methylether, TME, (8) as the main
2 reaction product. Other compounds were also identified in the complex reaction
3 mixture and the most important intermediates were identified as: (i) bi-cyclic
4 terpenes: camphene (9) and unreacted pinene (1); (ii) monocyclic terpenes: limonene
5 (5), terpinolene (6) and terpinene (7), and (iii) bicyclic ethers (α -fenchyl methyl ether,
6 and bornyl methylethers).

7 In order to explain the formation of these intermediates, it is reasonable to assume that
8 protons generated by the polarization of water [5, 19, 20], or methanol [8], by the
9 small, highly-charged Al^{3+} -cations will protonate pinene (1), leading to the pinyl ion
10 (2). Another possibility is the generation of methoxonium ions from methanol, which
11 will act as the protonating agent of pinene, leading to the same pinyl ion (2). Then, the
12 acid-catalyzed process proceeds via two parallel pathways: (i) ring expansion, via the
13 bornyl ion (4), giving rise to bi- and tricyclic isomerization products (camphene, 9)
14 and, after the addition of methanol, to bicyclic ethers (methyl fenchyl ether, 10,
15 methyl bornyl ether, 11), and (ii) via the terpinyl ion (3), yielding monocyclic
16 terpenes as isomerization products (limonene, 5, terpinolene, 6, terpinene, 7) and
17 terpinyl methylethers as methoxylation products (terpinyl methylether, 8). This range
18 of intermediates and products conforms with the reaction scheme proposed by Pito *et*
19 *al.* [11, 12].

20

21 Scheme 1. The main reaction products and intermediates identified by GC-MS in the
22 reaction mixture.

23

24 A typical set of concentration versus time data, obtained for the alkoxylation of α -
25 pinene over Al-SAz-1 and Al-SD catalysts, is presented in Figure 4. This figure also

1 presents the yield of pinene and terpinyl methylether, as a function of time elapsed,
2 along with the content of the other products identified above. The solid lines linking
3 the decrease in α -pinene concentration at early times identify the ranges used for the
4 calculation of the initial reaction rates, estimated as described in the experimental
5 section.

6

7

8 Figure 4. The change in composition of the reaction mixture during pinene
9 methoxylation over (a), (b) AlSAz-1 and (c), (d) AlSD. Reaction conditions: 200 mg
10 catalyst, 10 ml methanol, 0.5 ml pinene, 60 °C.

11

12 The most important feature of this catalytic system was the high selectivity towards
13 the main product, α -terpinyl methyl ether, especially at high pinene conversions. This
14 behaviour contrasts with that of limonene alkoxylation, when high selectivity was
15 observed during the early stages of reaction and decreased at high limonene
16 conversions. The system studied here is of considerable practical importance because
17 it offers good selectivities towards the mono-ether (65%), even at high pinene
18 conversion (higher than 60%). Moreover, the Al^{3+} -clay catalysts were able to produce
19 these high yields in only 1 hr whereas other solid acids [11,12, 13] required up to 50
20 hours to produce similar results.

21 The data in Figure 4 clearly demonstrate that the catalytic activity was profoundly
22 influenced by the nature of the starting clay (SAz-1 or SD). Catalytic activities over
23 clays, whether they arise from Brønsted or Lewis acidity, generally correlate with the
24 cation-exchange capacity (CEC) of the base clay, provided the reactant can enter the
25 gallery. Thus, SAz-1, a well-known montmorillonite of relatively high CEC (120 meq

1 (100g clay)⁻¹), would provide more acid sites than a similarly exchanged SD sample
2 (CEC 81 meq (100g clay)⁻¹). The catalytic activities recorded in this reaction clearly
3 reflected the relative abundance of acid sites on the catalyst surface. Thus, for these
4 Al³⁺-exchanged clays the order of activities was the same as the order of acid site
5 concentrations, as determined by CHA desorption experiments (Table 2), which were
6 also related to the CEC of the selected clay.

7 The selectivity towards α -terpinyl methyl ether (Fig. 4) was similar, irrespective of
8 the nature of the host clay, suggesting that the same mechanism was operating in both
9 cases. This is consistent with the proposed model, with protons being produced from
10 water molecules that have been strongly polarized by the exchangeable Al³⁺-cations
11 present in the interlayer space of the clay [8,16,19,20].

12

13 *3.2.3 Influence of the thermal activation temperature*

14 Figure 5, which presents the pinene conversion over AlSAz-1 catalyst pretreated at
15 different temperatures, supported the generally accepted model that the acid character
16 of an Al³⁺-exchanged montmorillonite is strongly dependent on the thermal activation
17 procedure. The deliberately hydrated samples, displayed a very low catalytic activity,
18 suggesting that the acid sites were blocked by water making them inactive towards the
19 reactants. Increasing the pretreatment temperature to 80 and 100 °C caused a marked
20 increase in activity. The maximum Brønsted acidity was generated upon thermal
21 activation at 150 °C, as shown in the VT-DRIFTS spectra of the pyridine treated Al³⁺-
22 clays, but only a slight increase in activity was observed at this temperature.

23 Increasing the thermal activation temperature above 150 °C, is known to cause a
24 reduction in the Brønsted acidity and an increase in the Lewis acidity in accordance
25 with the model in which the exchange ions become electron pair accepting, or Lewis

1 acid, sites as the directly coordinated water is driven off [16]. Therefore, a
2 pretreatment temperature of 150 °C was selected for further studies, in order to avoid
3 the uncertainty regarding the Brønsted/Lewis acid balance and to take advantage of
4 the maximum number of the Brønsted acid sites.

5
6 Figure 5. The effect of the Al-clay activation temperature on the methoxylation of α -
7 pinene: (A) α -pinene conversion vs. time and (B) the correlation selectivity vs.
8 conversion. Reaction conditions: 200 mg cat, 10 ml methanol, 0.5 ml pinene, 60 °C.

9
10 The variation of selectivity towards terpinyl methylether, TME, with the extent of
11 pinene conversion was also scrutinized. The data in Figure 5B clearly illustrate that
12 the activation temperature exerted little influence on selectivity, especially at low
13 pinene conversion. Therefore, while the activation temperature exerted a considerable
14 effect on the reaction rate, the selectivity toward TME was not influenced in any
15 significant way.

16 *3.2.4 Influence of the reaction temperature*

17 The influence of the reaction temperature on pinene conversion and selectivity
18 towards the mono-ether is presented in figures 6A and 6B. The catalysed reactions
19 were carried out at different temperatures (35, 45, 55 and 65 °C) over 100 mg of Al-
20 SAz-1 catalyst while the pinene : methanol molar ratio and the catalyst loading were
21 kept constant. As anticipated, pinene conversion increased with the temperature,
22 under otherwise identical conditions. The same trend was observed for limonene
23 conversion in a related system [8]. Increasing the temperature up to 65 °C, did not
24 lead to a decrease in selectivity, as observed in the previous study on limonene
25 methoxylation [8]. The selectivity to the mono-ether (Figure 6), at constant

1 conversion, seems to be largely unaffected by raising the reaction temperature.

2

3 Figure 6. The effect of the reaction temperature on the methoxylation of α -pinene:

4 (A) α -pinene conversion vs. time and (B) the correlation selectivity vs. conversion.

5 Reaction conditions: 100 mg Al-SAz-1, 0.5 ml Pinene, 10 ml MeOH.

6

7 3.2.5 Influence of initial α -pinene concentration

8 The effect of the initial α -pinene concentration on the conversion and on the

9 selectivity towards the mono-ether is presented in Figure 7. Doubling the initial

10 pinene concentration, from 0.3 to 0.6 mol/L, only caused a slight decrease in pinene

11 conversion at a fixed reaction time; this trend was further accentuated at a higher

12 initial concentration (1.05 mol/L). Note that the initial reaction rate was higher when

13 the initial concentration of pinene was higher, under otherwise identical conditions.

14 Again, the selectivity to the mono-ether, at similar conversion, was not affected by the

15 initial pinene concentration.

16

17 Figure 7. The effect of the initial pinene concentration on the methoxylation of α -

18 pinene: (A) α -pinene conversion vs. time and (B) the correlation selectivity vs.

19 conversion. Reaction conditions: 200 mg catalyst, 10 ml methanol, 60 °C.

20

21 3.3 Kinetic study

22 The linear form of the logarithmic plot of α -pinene concentration *versus* time,

23 demonstrated that the reaction over the clay catalysts followed pseudo first-order

24 kinetics; i.e. first order with respect to α -pinene and zero-order with respect to

25 methanol, because the latter was present in large excess. The values of the reaction

1 rate constants, determined from the slopes of the two lines of negative slope in Figure
2 8, confirmed that the rate of reaction at 60 °C was faster over Al-SD than Al-SA_z.

3

4 Figure 8. α -pinene concentration versus time during the methoxylation of α -pinene
5 over AlSA_z-1 and AlSD. Reaction conditions: 200 mg catalyst, 10 ml methanol, 0.5
6 ml pinene, 60 °C.

7

8 An Arrhenius plot of these reaction rate constants is shown Figure 9. The slopes of the
9 $\ln r$ versus $1/T$ lines were similar for both Al-exchanged clays, and an activation
10 energy of 71.7 kJ/mole was obtained for the alkoxylation reaction.

11

12 The similarity in activation energies suggested that the difference in rate constants
13 must be attributed to a difference in the pre-exponential factor. An acceptable
14 explanation for the faster rate over AlSD is that the significantly higher external
15 surface area makes it easier for the reactant and product molecules to arrive at the
16 Brønsted acid sites in the gallery. This suggests that the rate determining step involves
17 transport from the liquid phase to the interlayer space perhaps via a 'stagnant' layer of
18 reaction medium close to the clay surface. Alternatively, the larger distance between
19 exchange sites in AlSD, which has a lower density of exchange sites per unit surface,
20 may control or contribute to easier access to the reaction sites in the clay interlayer.
21 The high charge density of the AlSA_z sample may result in interlayer congestion
22 which results in a slower rate of turnover at the acid sites.

23

24 Figure 9. Arrhenius plot for methoxylation of α -pinene over AlSA_z-1 and AlSD.

25 Reaction conditions: 100 mg catalyst, 10 ml methanol, 0.5 ml pinene.

1

2 4. Conclusion

3 Modified clays have been proposed as active and selective catalysts for the synthesis
4 of α -terpinyl methyl ether by alkoxylation of α -pinene with methanol. The GC-MS
5 analysis of the reaction mixtures showed that α -terpinyl methyl ether was obtained
6 with good selectivity over the Al^{3+} -exchanged clay catalysts. AlSAz-1 was
7 significantly more active than the similarly exchanged SD, and this behaviour was
8 rationalized taking into account the higher number of Brønsted acid sites present in
9 this high charge clay, as shown by the acidity measurements (VT-DRIFTS and TG of
10 CHA). The activation temperature had a strong influence on the acidity of the clay
11 surface and was, consequently, a significant factor in the control of the reaction rate.
12 In addition, other reaction parameters, such as the reaction temperature and the initial
13 concentration of α -pinene could be used to optimize the catalytic activity. The
14 selectivity towards the mono-ether at constant conversion was much less dependent
15 on these parameters.

16 The most important feature of this catalytic system was the high selectivity towards
17 the main product, α -terpinyl methyl ether, especially at high pinene conversions. In
18 this sense, the selectivity towards TME (65%), obtained over Al^{3+} -exchanged clays, is
19 similar to that obtained by Pito et al. [11, 12] and Mato et al. [13] (60%) but at a much
20 higher reaction rate. On the other hand, Hoelderich [7] suggested that zeolite β is
21 more active than the clay-based catalysts, at the expense of the selectivity, which is
22 significantly poorer (54%), especially at high conversions. A different trend was
23 observed in the related alkoxylation of limonene, over the same catalysts, where the
24 selectivity decreased as the limonene conversion progressed. The reaction followed
25 pseudo first-order kinetics, with similar activation energies for both catalysts.

1

2 **5. Acknowledgements**

3 This work was supported by Portuguese funds (FCT - Fundação para a Ciência e a
4 Tecnologia, projects PTDC/CTM-CER/121295/2010 and PEst OE/QUI/UI0619/2011)

5 **6. References**

6 [1] P. T. Anastas, L. B. Bartlett, M. M. Kirchhoff, and T. C. Williamson, *Catal.*

7 *Today* 55 (2000) 11–22

8 [2] Noma Y, Asakawa Y (2010). Biotransformation of monoterpenoids by

9 microorganisms, insects, and mammals. In: Baser KHC, Buchbauer G (eds).

10 Handbook of Essential Oils: Science, Technology, and Applications. CRC Press:

11 Boca Raton, 585–736.

12 [3] E.V. Gusevskaya, *ChemCatChem*. 6 (2014) 1506-1515

13 [4] M. Besson, P. Gallezot and C. Pinel, *Chem. Rev.*, 114 (2014) 1827-1870

14 [5] A. Corma, S. Iborra, and A. Velty, *Chem. Rev.* 107 (2007) 2411–2502

15 [6] P. Mäki-Arvela, B. Holmbom, T. Salmi, and D. Y. Murzin, *Cat. Rev.* 49 (2007)

16 197–340

17 [7] K. Hensen, C. Mahaim, and W. F. Hölderich, *Appl. Catal. A: General* 149 (1997)

18 311–329

19 [8] C. Catrinescu, C. Fernandes, P. Castilho, C. Breen, M. M. L. Carrott, and I. P. P.

20 Cansado, *Appl. Catal. A: General* 467 (2013) 38–46

21 [9] M. Yoshiharu and M. Masahiro, *Jpn. Kokai*, 75 (1976) 948

22 [10] J. E. Castanheiro, L. Guerreiro, I. M. Fonseca, A. M. Ramos, and J. Vital

23 *Stud. Surf. Sci. Catal.* 174 (2008) 1319-1322

24 [11] D. S. Pito, I. M. Fonseca, A. M. Ramos, J. Vital, and J. E. Castanheiro, *Chem.*

25 *Eng. J.* 147 (2009) 302–306

- 1 [12] D. S. Pito, I. Matos, I. M. Fonseca, A. M. Ramos, J. Vital, and J. E. Castanheiro,
2 *Appl. Catal. A: General.* 373 (2010) 140–146
- 3 [13] I. Matos, M. F. Silva, R. Ruiz-Rosas, J. Vital, J. Rodríguez-Mirasol, T. Cordero,
4 J. E. Castanheiro, I. M. Fonseca, *Micropor. Mesopor. Mat.* (199) 2014 66-73
- 5 [14] J. M. Adams and R. W. McCabe, “Chapter 10.2 Clay Minerals as Catalysts,” in
6 *Handbook of Clay Science*, vol. 1, Elsevier, 2006, 541–581
- 7 [15] F. Bergaya, B. K. G. Theng, and G. Lagaly, “Chapter 7 Modified Clays and
8 Clay Minerals,” in *Handbook of Clay Science*, vol. 1, Elsevier, 2006, p261.
- 9 [16] C. Breen, *Clay Miner.* 26 (1991) 473–486
- 10 [17] L. J. Arroyo, H. Li, B. J. Teppen, and S. A. Boyd, *Clays Clay Miner* 53
11 (2005) 512 – 520
- 12 [18] S. Kaufhold, R. Dohrmann, M. Klinkenberg, S. Siegesmund, and K. Ufer,
13 *Journal of Colloid and Interface Science* 349 (2010) 275–282
- 14 [19] C. Breen, *Clay Miner.* 26 (1991) 487–496
- 15 [20] P. Komadel, M. Janek, J. Madejova, A. Weekes, and C. Breen, *J. Chem. Soc.*
16 *Faraday Trans.* 93 (1997) 4207–4210
- 17 [21] T. K. Sherwood, *Pure and Appl. Chem.* 10 (1965) 595–610
- 18 [22] H. Hichri, A. Accary, and J. Andrieu, *Chem. Eng. Process.* 30 (1991) 133–
19 140
- 20 [23] S. Brunauer, P. H. Emmett and E. Teller, *J. Am. Chem. Soc.*, 60 (1938) 309-319
21

1 **Figure captions**

2 Figure 1. The powder XRD patterns for raw, purified and Al³⁺-exchanged clays.

3 Impurities: magnesian calcite (C), anorthite (A), feldspar (F) and quartz (Q)

4 Figure 2 . VT-DRIFTS spectra of Al-SAz-1 following exposure to pyridine vapour
5 and evacuation at (a) 50 °C, (b) 100 °C, (c) 150 °C, (d) 200 °C and (e) 250 °C.

6 Figure 3. The influence of the catalyst load on the initial reaction rate over AlSAz-1
7 and AlSD. Inset: Early time behaviour. Reaction conditions: 10 ml methanol, 0.5 ml
8 pinene, 60 °C, 750 rpm

9 Scheme 1. The main reaction products and intermediates identified by GC-MS in the
10 reaction mixture.

11 Figure 4. The change in composition of the reaction mixture during pinene
12 methoxylation over (a), (b) AlSAz-1 and (c), (d) AlSD. Reaction conditions: 200 mg
13 catalyst, 10 ml methanol, 0.5 ml pinene, 60 °C.

14 Figure 5. The effect of the Al-clay activation temperature on the methoxylation of α-
15 pinene: (A) α-pinene conversion vs. time and (B) the correlation selectivity vs.
16 conversion. Reaction conditions: 200 mg cat, 10 ml methanol, 0.5 ml pinene, 60 °C.

17 Figure 6. The effect of the reaction temperature on the methoxylation of α-pinene:
18 (A) α-pinene conversion vs. time and (B) the correlation selectivity vs. conversion.
19 Reaction conditions: 100 mg Al-SAz-1, 0.5 ml Pinene, 10 ml MeOH.

20 Figure 7. The effect of the initial pinene concentration on the methoxylation of α-
21 pinene: (A) α-pinene conversion vs. time and (B) the correlation selectivity vs.
22 conversion. Reaction conditions: 200 mg catalyst, 10 ml methanol, 60 °C.

23 Figure 8. α-pinene concentration versus time during the methoxylation of α-pinene
24 over AlSAz-1 and AlSD. Reaction conditions: 200 mg catalyst, 10 ml methanol, 0.5
25 ml pinene, 60 °C.

- 1 Figure 9. Arrhenius plot for methoxylation of α -pinene over AlSAz-1 and AlSD.
- 2 Reaction conditions: 100 mg catalyst, 10 ml methanol, 0.5 ml pinene.
- 3

Figure 1

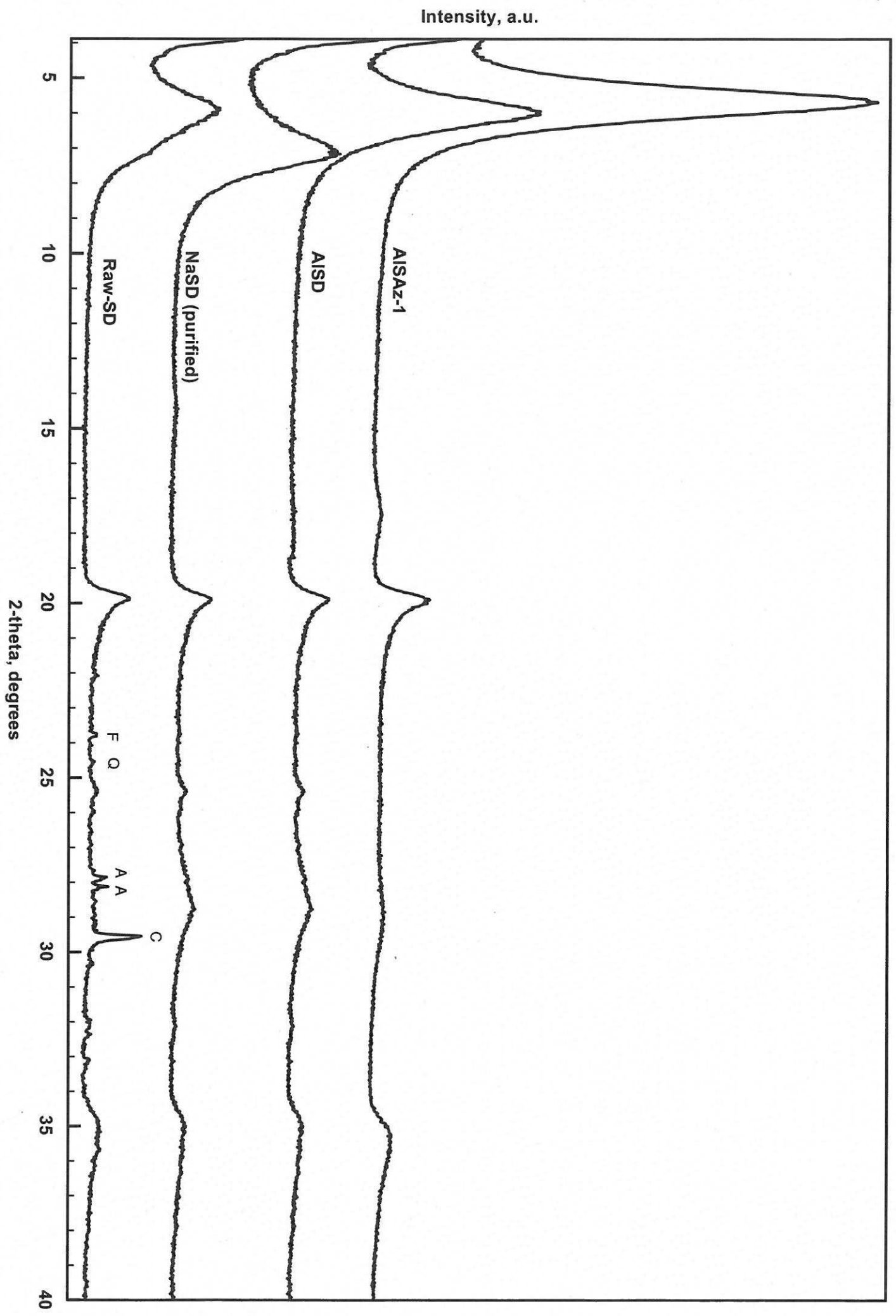


Figure 2

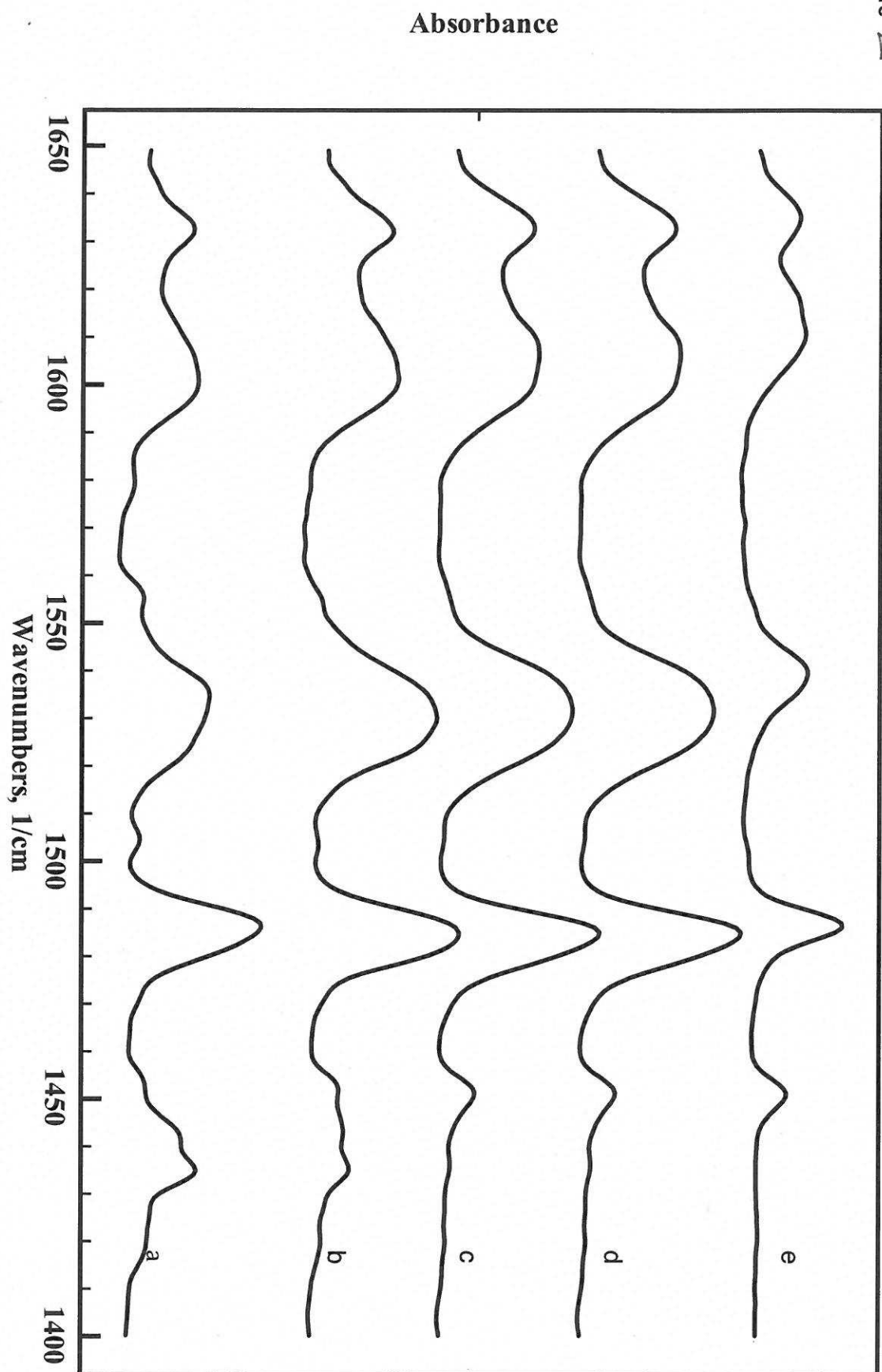


Figure 3

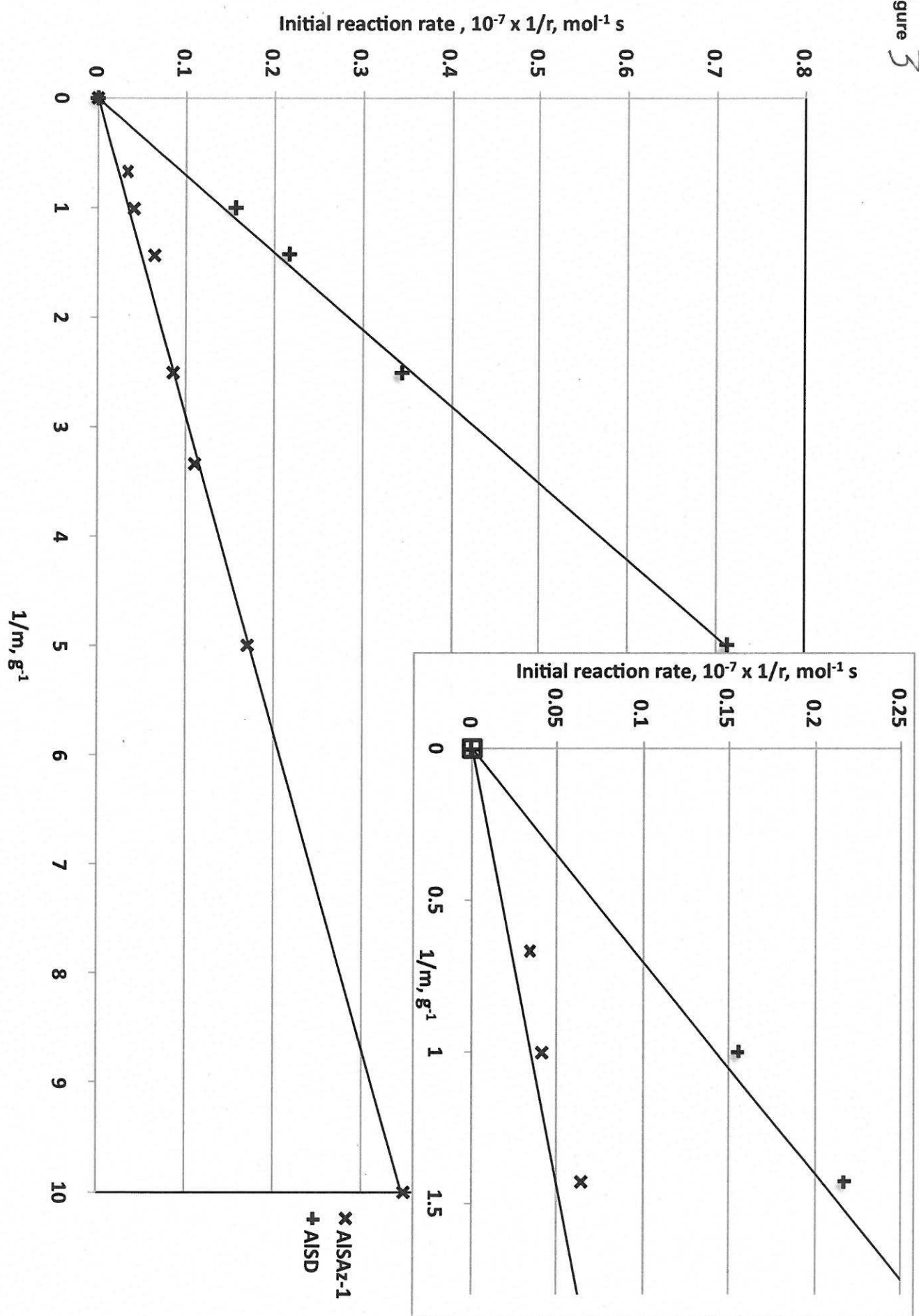
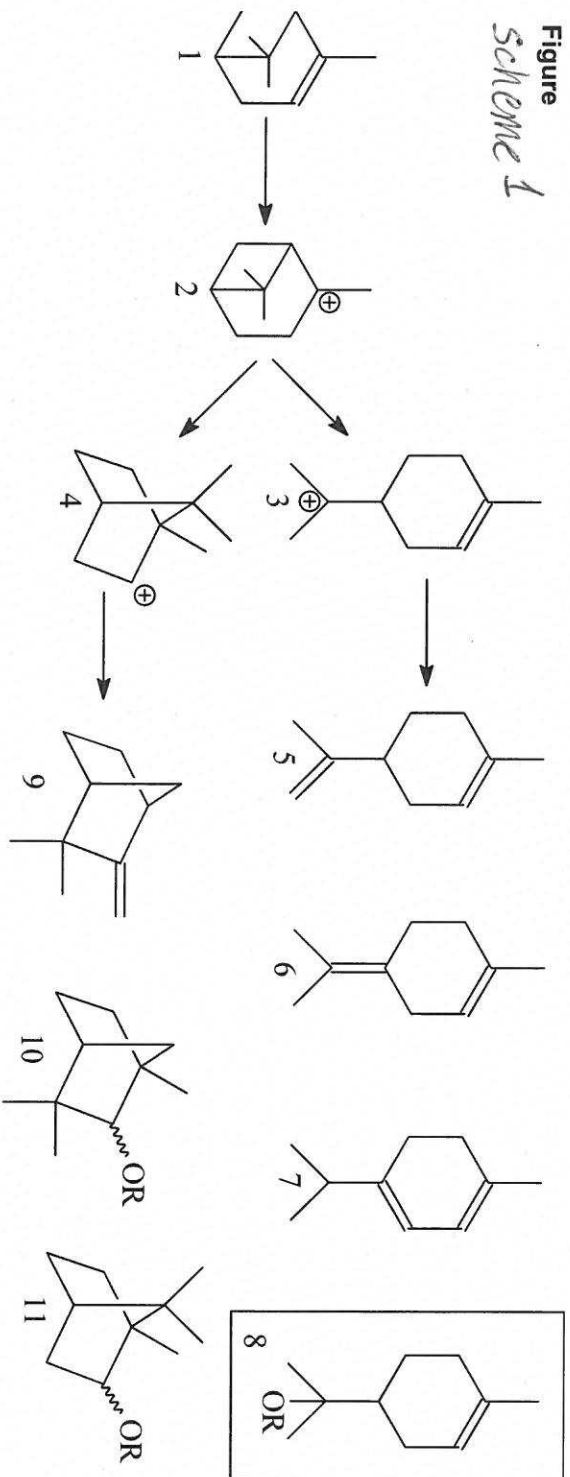


Figure
Scheme 1



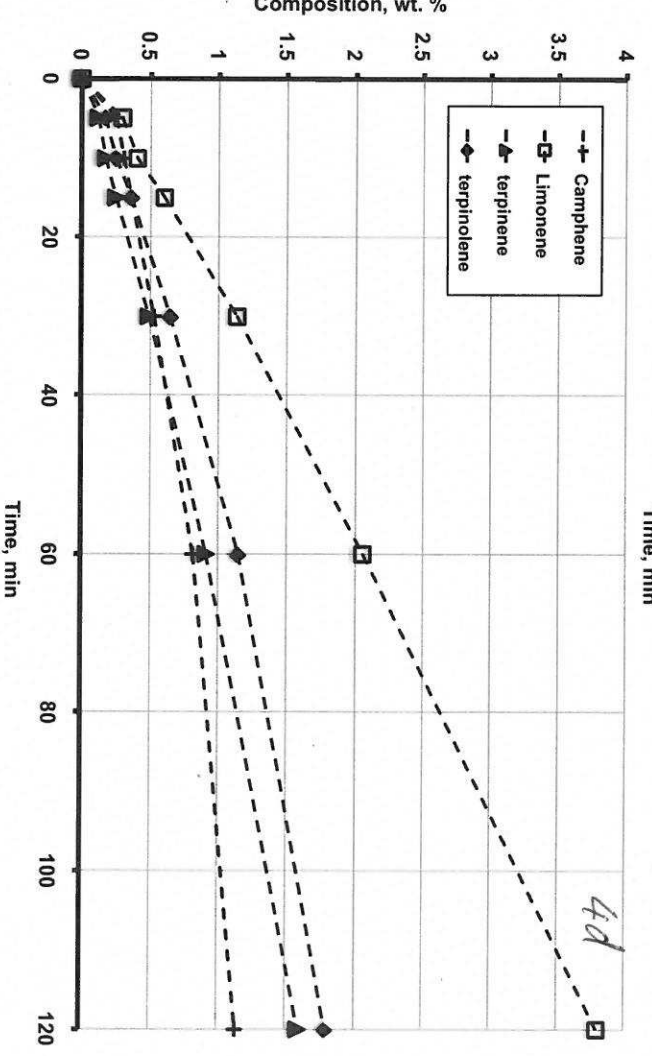
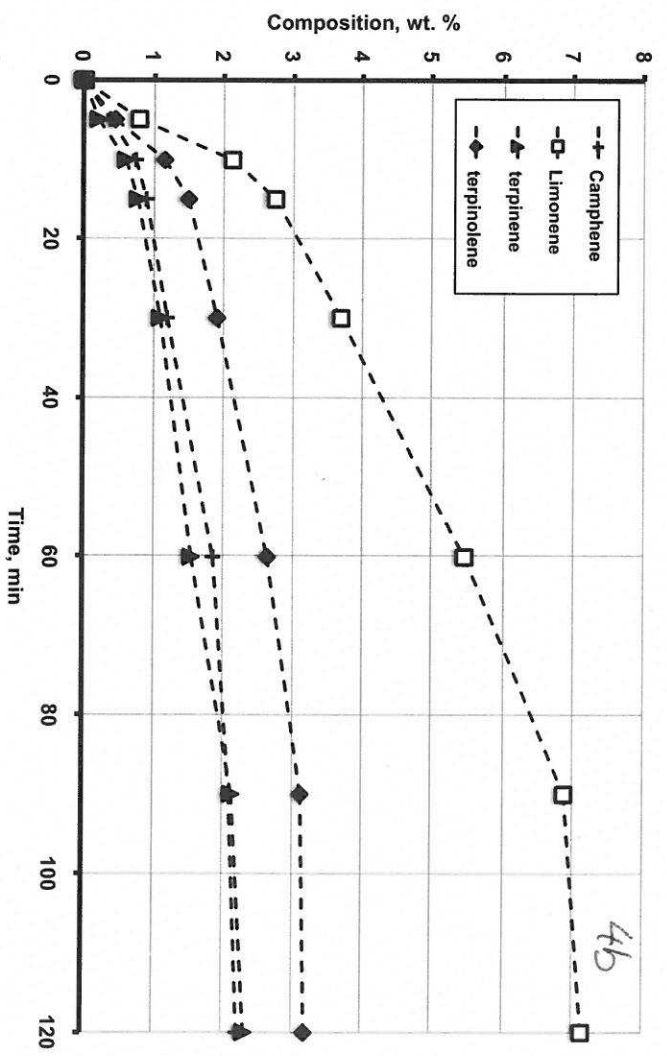
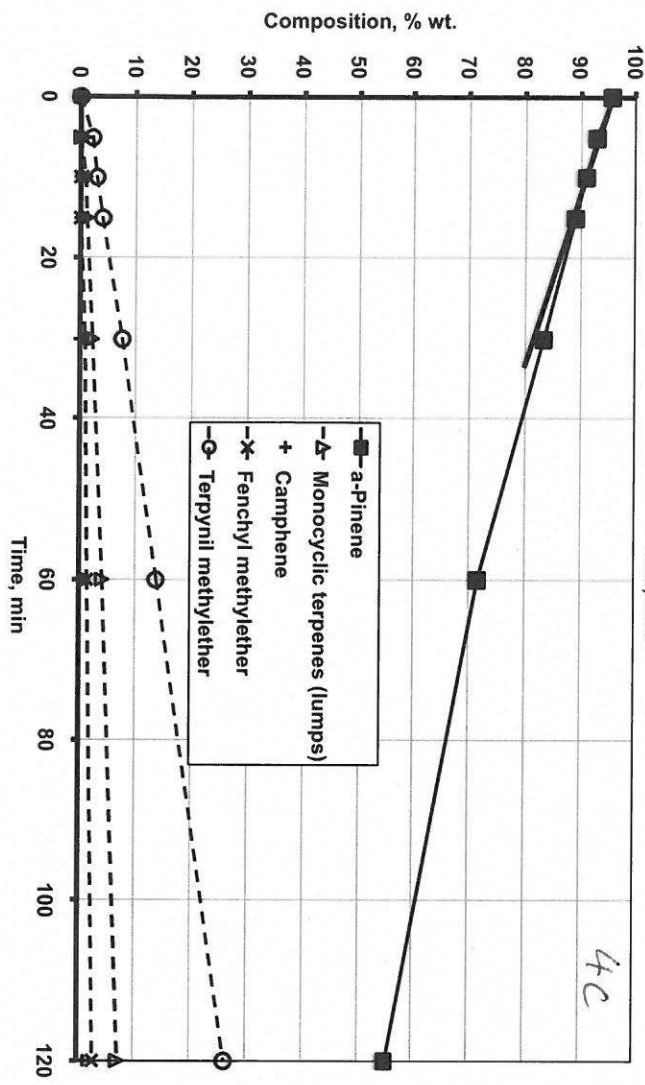
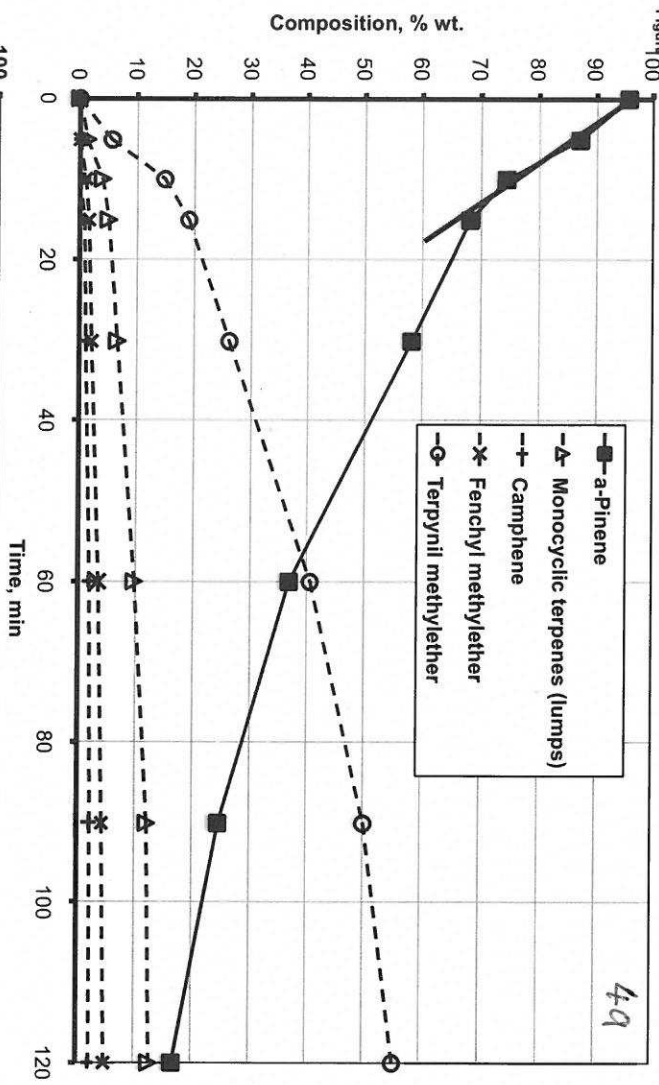
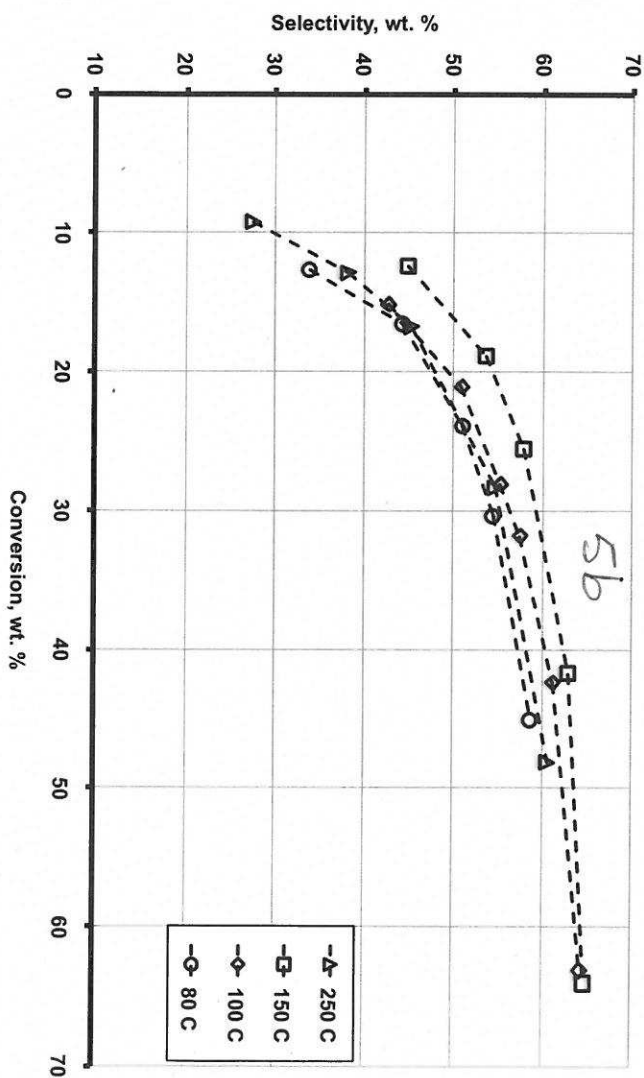
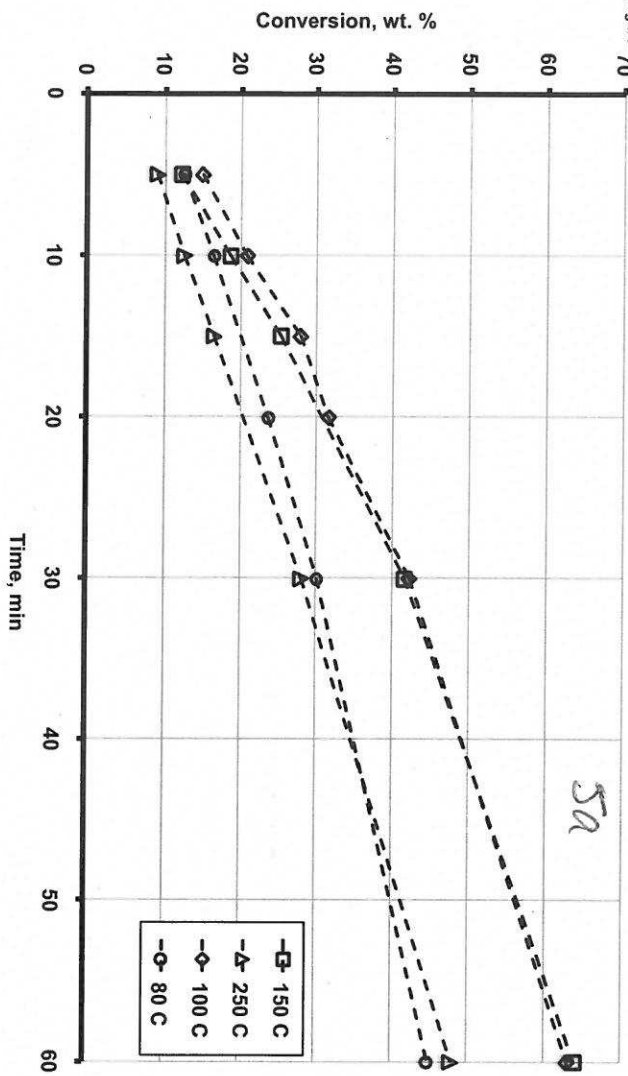
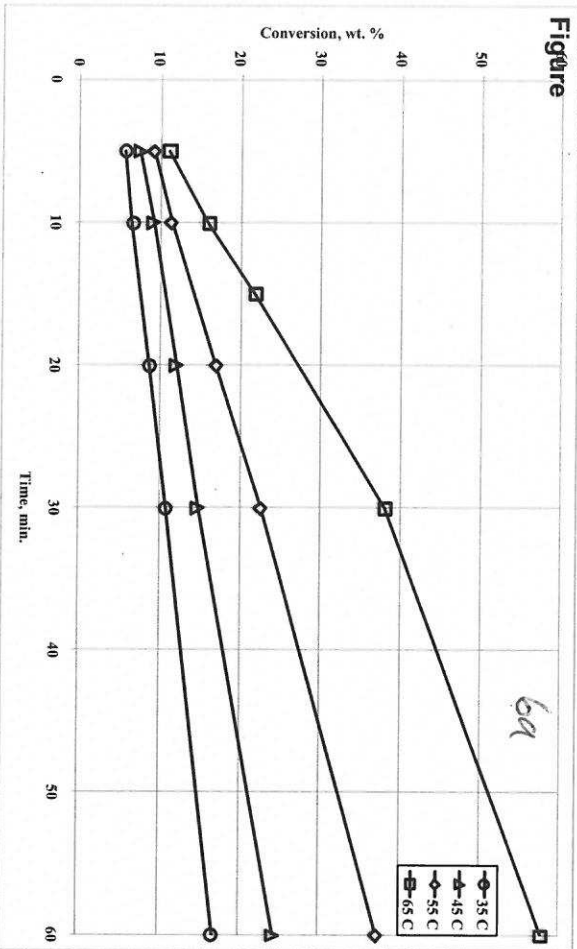


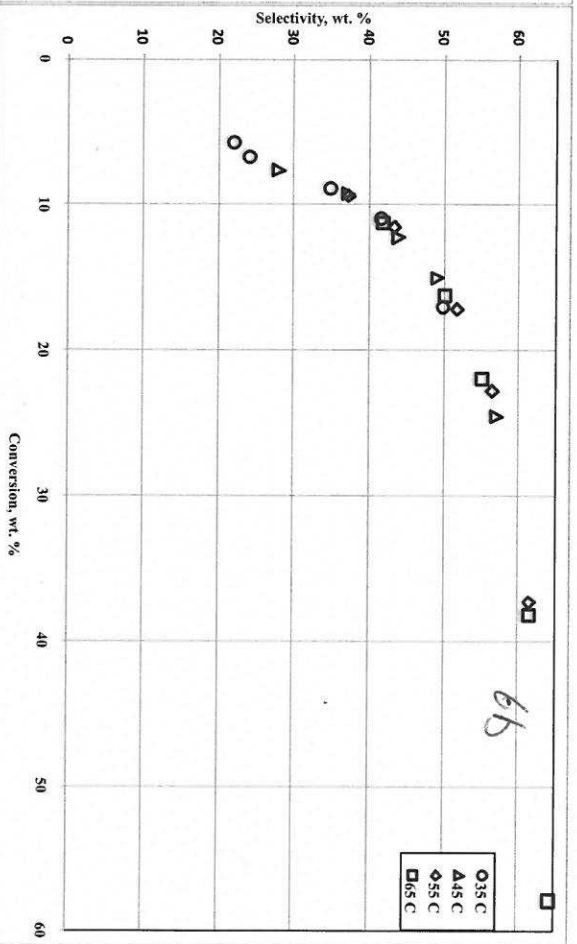
Figure 70



Figure



6a



6b

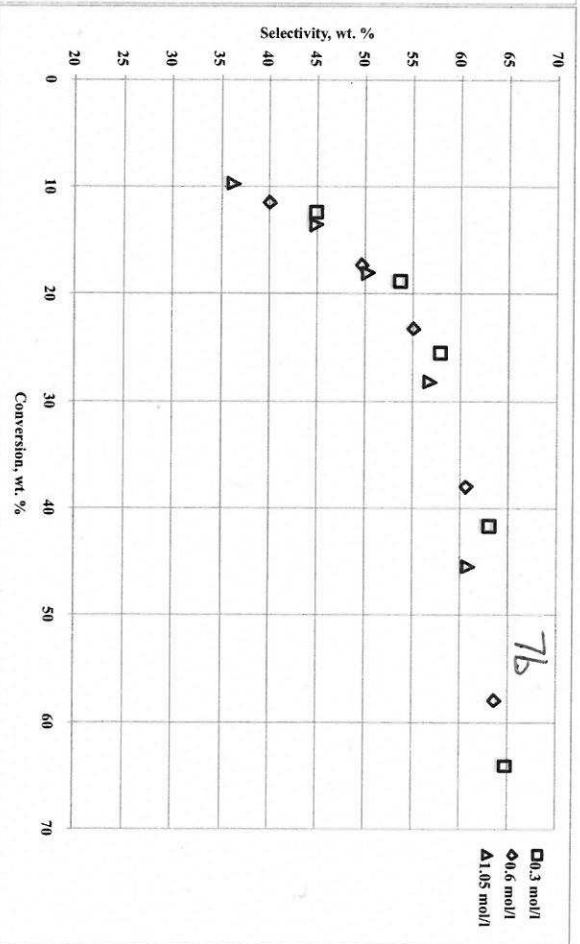
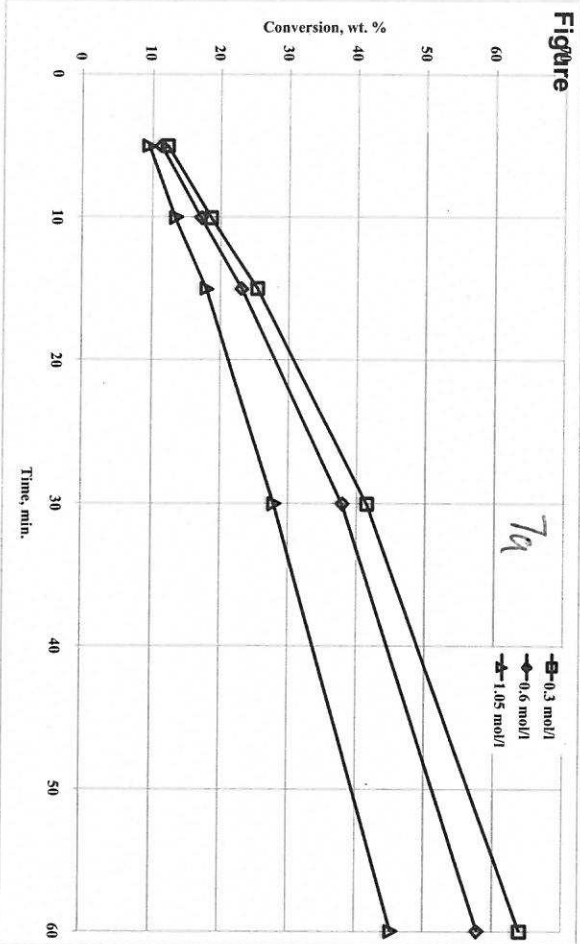
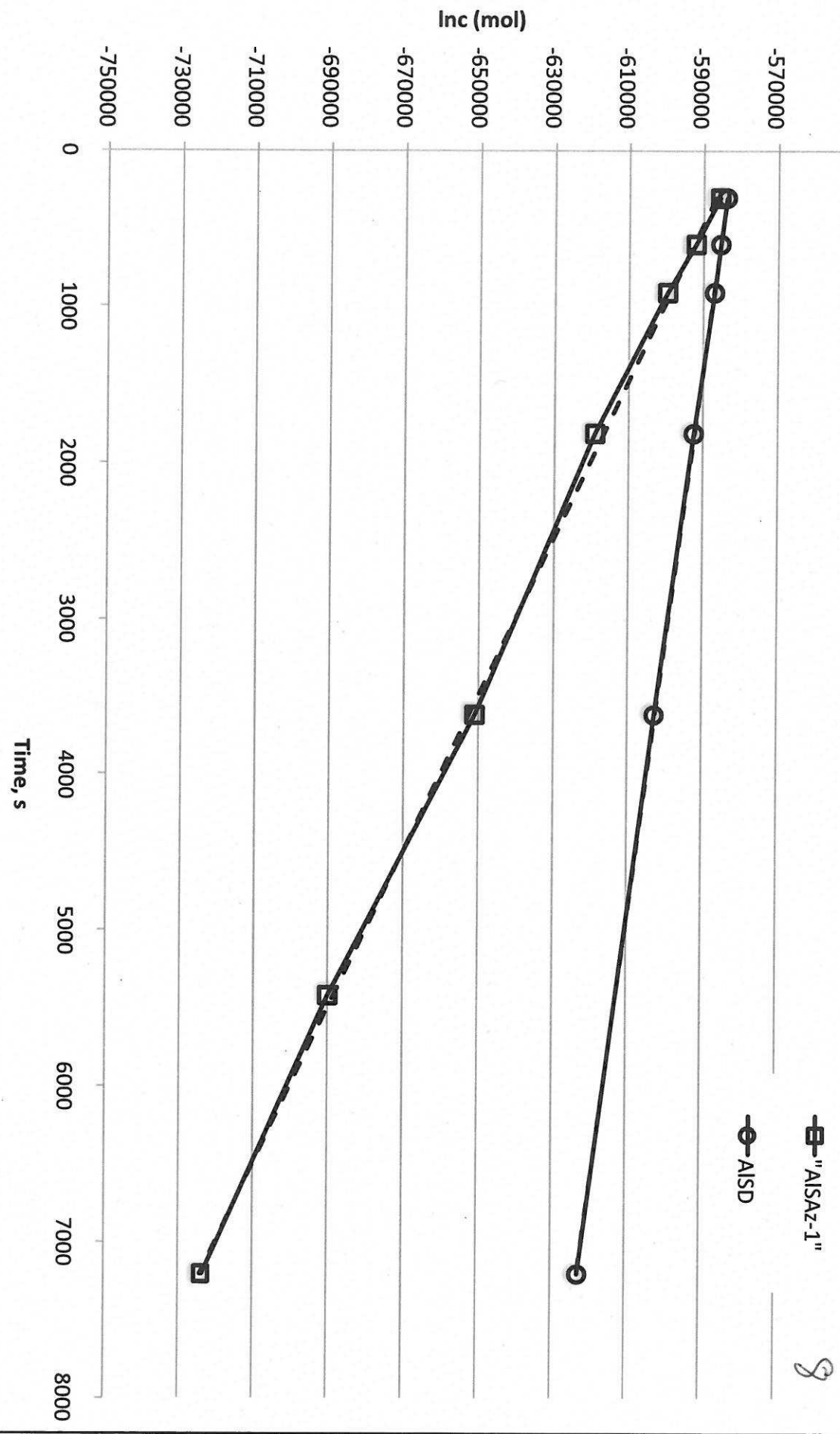
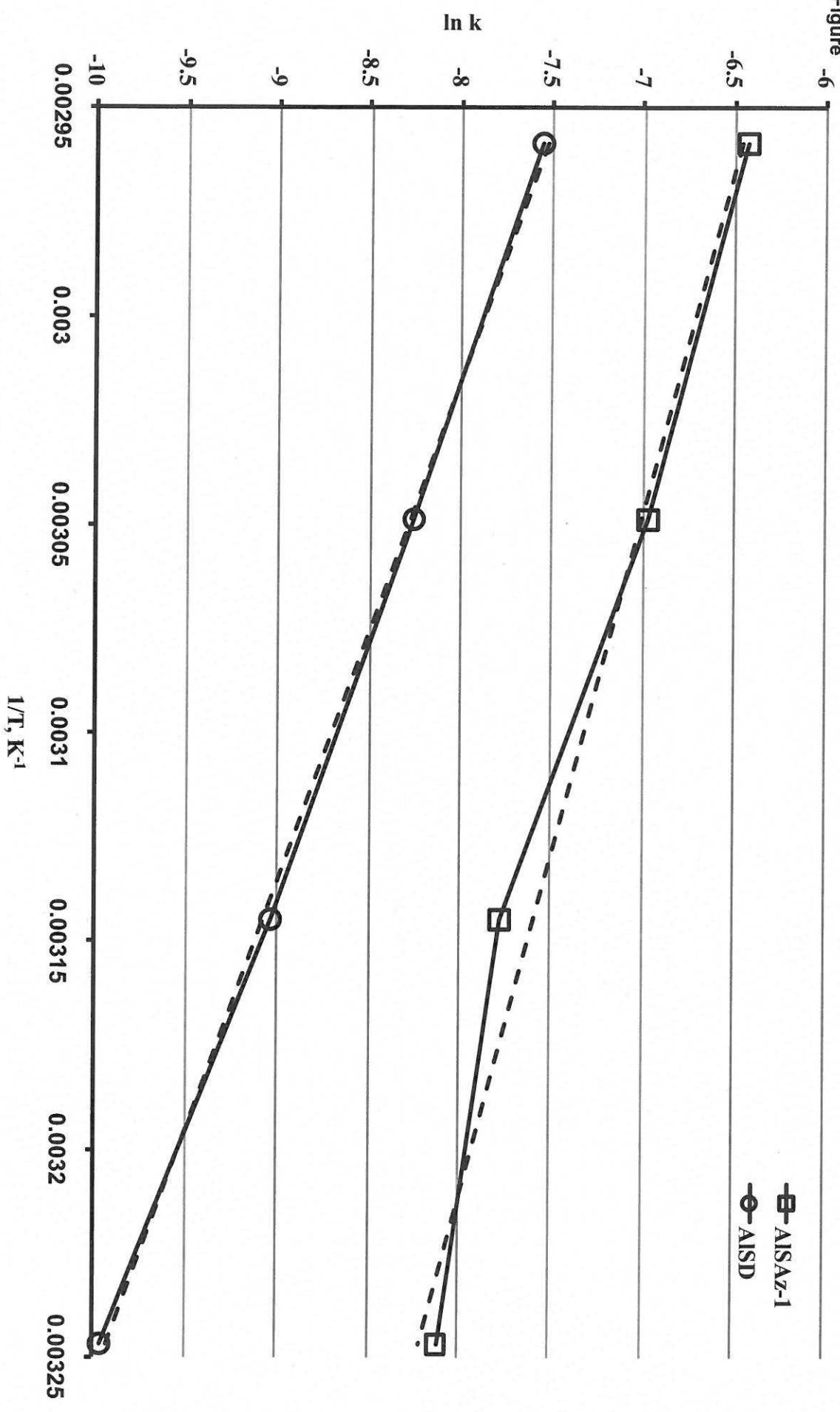


Figure -550000



8

Figure -6



Supplementary Material

[Click here to download Supplementary Material: Supplementary.pdf](#)

